IEEE Access
Multidisciplinary | Rapid Review | Open Access Journal

Received January 7, 2018, accepted February 17, 2018, date of publication February 23, 2018, date of current version March 15, 2018.

Digital Object Identifier 10.1109/ACCESS.2018.2808335

Novel Surface Plasmon Polariton Waveguides with Enhanced Field Confinement for Microwave-Frequency Ultra-Wideband Bandpass Filters

YING JIANG GUO[1], (Student Member, IEEE), KAI DA XU[2,3], (Member, IEEE), YANHUI LIU[2], (Member, IEEE), AND XIAOHONG TANG[1]

[1]EHF Key Laboratory of Science, University of Electronic Science and Technology of China, Chengdu 611731, China
[2]Department of Electronic Science, Xiamen University, Xiamen 361005, China
[3]Shenzhen Research Institute, Xiamen University, Shenzhen 518057, China

Corresponding author: Kai Da Xu (kaidaxu@xmu.edu.cn)

This work was supported in part by the National Natural Science Foundation of China under Grant 61601390 and in part by the Shenzhen Science and Technology Innovation Project under Grant JCYJ20170306141249935.

ABSTRACT In this paper, a novel planar waveguide based on spoof surface plasmon polaritons (SSPPs) using fish-bone corrugated slot structure is first proposed in the microwave region. Low-dispersion band can be realized by such structure with tight field confinement of SSPPs, resulting in size miniaturization of the proposed waveguide. The high frequency stopband of the proposed ultra-wideband bandpass filter (BPF) is created by using this proposed waveguide, while the low frequency stopband is properly designed through introducing the microstrip-to-slotline transition. The 2-D E-fields distribution, surface current flow, and energy flow patterns are all calculated and illustrated to demonstrate the electromagnetic (EM) characteristics of the proposed ultra-wideband BPF. The BPF tuning characteristics is explored to provide a guideline for facilitating the design process. To validate the predicted performance, the proposed filter is finally designed, fabricated, and measured. Measured results illustrate high performance of the filter, in which the reflection coefficient is better than −10 dB from 2.1 to 8 GHz with the smallest insertion loss of 0.37 dB at 4.9 GHz, showing good agreement with numerical simulations. The proposed surface plasmon polariton waveguides are believed to be significantly promising for further developing plasmonic functional devices and integrated 2-D circuits with enhanced confinement of SSPPs in microwave and even terahertz bands.

INDEX TERMS Bandpass filter, surface plasmon polaritons, ultra-wideband.

I. INTRODUCTION

Surface plasmon polaritons (SPPs) are surface electromagnetic (EM) waves propagating on the metal-dielectric interface inspired by the coupling between free electrons in a metal and incident EM waves [1]. The EM energy will be confined tightly in subwavelength scale at visible frequencies and will be greatly enhanced with good modal shape and low propagation loss [2], [3]. Due to this characteristic, SPPs open up a previously inaccessible length scale for the optical research, which implies the possibility to use SPPs for the high sensitive biochemical sensors [4], miniaturized photonic circuits [5], and high-resolution imaging [6]. However, natural SPPs effect can only exist for applications at the intrinsic plasma frequency of metal which approaches the optical frequency. This is because, for most metals, the plasma frequencies corresponding to the intrinsic electron oscillation in a metal is usually located in the optical and even ultraviolet regions [7]. While at much lower frequency band (e.g., microwave and terahertz), deep subwavelength effect of SPPs cannot be realized due to the disability of internal plasmonic oscillations in metal, which severely restricts SPPs practical applications in microwave or terahertz regimes.

To solve this problem, the concept of SSPPs with periodical textures on the metal structures is firstly reported in 2004 to achieve deep subwavelength effect at microwave and terahertz frequencies [8]. The surface waves supported by these structures were named as designer SPPs or spoof SPPs (SSPPs) due to their mimicking characteristics.

Based on this concept, various kinds of plasmonic structures have been proposed and experimentally demonstrated for steering highly localized SSPPs waves in microwave and terahertz regimes in the last few years, such as one-dimensional (1-D) groove arrays [9], two-dimensional (2-D) hole lattices [10], and even conformal plasmonic structures [11]. These plasmonic structures not only have advantages of strong field confinement as that of optical SPPs, but also show the dispersion property with cutoff frequency of nature SPPs. Importantly, the SSPPs dispersion characteristics can be directly manipulated by tailoring the shapes and dimensions on patterns, providing an effective method to guide and control subwavelength routing of microwave and terahertz radiations. Unfortunately, these early plasmonic devices have an obviously disadvantage of inherent bulk three-dimensional geometrics and some even require complicated manufacturing techniques in fabrication process, which rigorously limits their practical applications.

Recently, ultrathin corrugated metallic strips design was presented to support SSPPs wave propagation on the thin planar paths, which have attractive features of smaller area compared with the bulk plasmonic structures [12]. Meanwhile, due to its good field confinement, the crosstalk from adjacent pairs of corrugated ultrathin waveguides is much lower than conventional microstrip pairs [13]. Because of these advantages, a series of passive and active devices based on planar SSPPs including antennas, amplifiers, filters and circulators have been proposed in order to construct SSPPs based circuits and systems with high performance [14]–[24].

In this paper, a novel high-performance microwave SSPPs waveguide engineered on ultrathin corrugated metallic strips is proposed. The presented plasmonic unit cell with lower dispersion band improves the confinement ability of SSPPs waves compared with the traditional unit cell [25]. Since such structure topology is unique and resembles fish bones, we call it fish-bone slot unit cell. Based on this structure, an ultra-wideband BPF with low reflection and high transmission coefficient for SSPPs waves is designed and fabricated. Introducing the presented artificial plasmonic unit cell, we can confine the microwave energy tightly with little propagation loss and generate the high frequency stopband for the passband. Also, to reach a perfect momentum matching between the SSPPs waveguide and the signal input port, a microstrip-to-slotline transition section and two fish-bone slot unit cells with different groove depths are designed for high-efficiency conversion. The designed transition also blocks the DC and low frequency signals, which is helpful to shape the passband by suppressing the DC and low frequency noise. Numerical simulations and experimental results demonstrate excellent performance of the proposed SSPPs waveguide and filter in ultra-wide frequency band, which builds a solid avenue for advanced plasmonic functional devices and circuits in microwave and terahertz devices.

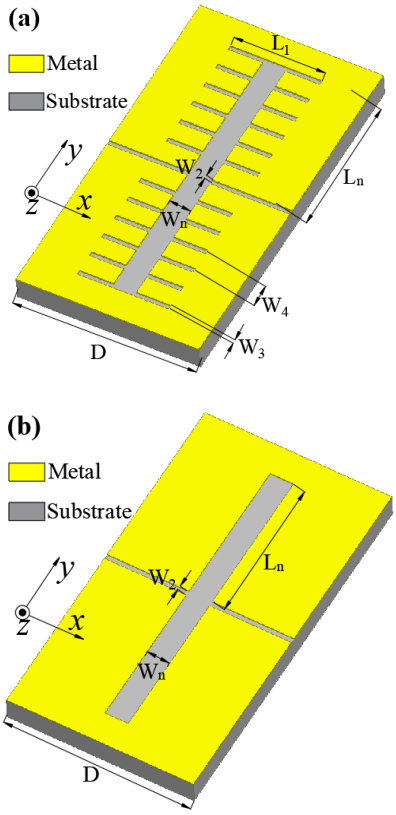

FIGURE 1. Schematic of (a) the proposed fish-bone slot unit cell and (b) the traditional slot unit cell.

II. DISPERSION CHARACTERISTICS OF THE PROPOSED FISH-BONE SLOT STRUCTURE

The schematic configuration of the fish-bone slot unit cell is depicted in Fig. 1(a), which will be periodically machined into a metal film on the bottom layer of dielectric substrate to form the SSPPs waveguide. The proposed groove is composed of mirror-oriented corrugated slots with lattice constant or period D, in which compound metallic geometry is further designed. The compound slot structure resembles fish bones consisting of main slots and subsidiary slots, where the subsidiary slots are paralleled with the signal transmission slotline and symmetrically arranged on the two sides of the main slots, as can be referred to Fig. 1(a). The compound slot structure is characterized by the widths and depths of these two kinds of slots (i.e., W_n, W_3, L_n, L_1), and the pitch between the subsidiary slots of W_4.

The dispersion curves are obtained by theoretical calculations and numerical eigen-mode simulations, which are carried out by the commercial software, CST Microwave Studio. To simplify the analysis, the metal is assumed to be perfect electric conductor (PEC). The dispersion characteristics of periodic arrangement of fish-bone slot unit cell are investigated by placing the proposed slot unit cell in an air box where the boundaries in the x direction should be set as the periodic boundary, and the other boundaries in the y and z directions

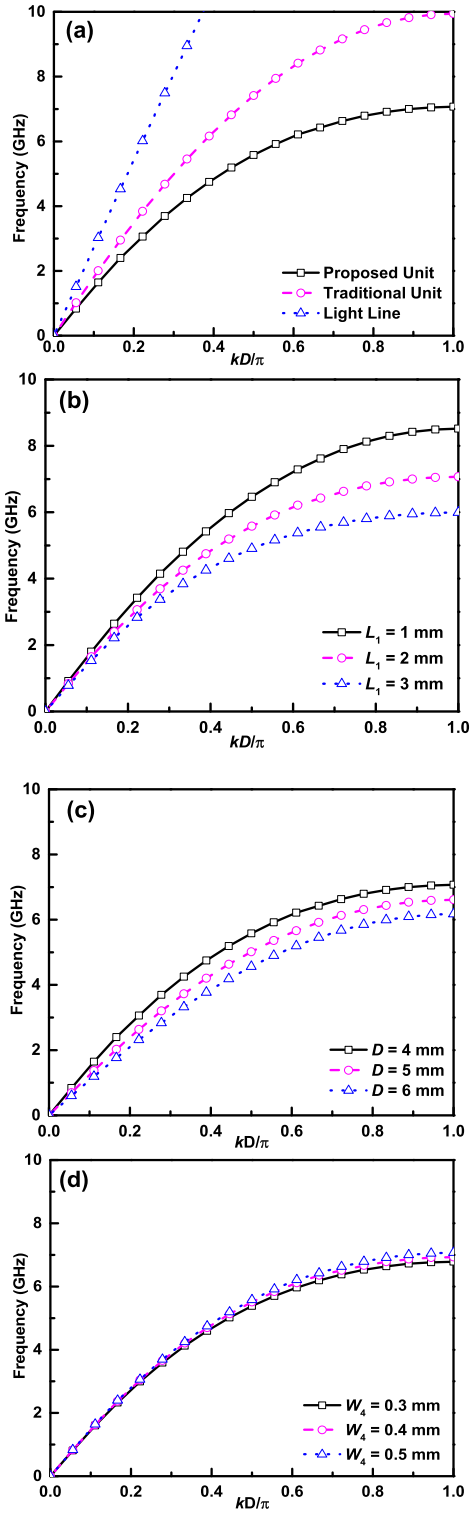

FIGURE 2. **(a) Dispersion curves of the proposed slot unit cell, traditional slot unit cell and light line. The physical parameters L_n, W_n, L_1, W_2, W_3, W_4 and D are chosen as 3 mm, 0.5 mm, 2 mm, 0.2 mm, 0.1 mm and 0.5 mm, respectively. Dispersion curves of the proposed fish-bone slot unit cell with different values of (b) L_1, (c) D and (d) W_4.**

are set as the PEC boundary. All eigen-frequencies are calculated when sweeping the phase difference between the two periodic boundaries from 0° to 180°. Thus, the dispersion relation is obtained. For all cases in this paper, the substrate is with dielectric constant of 3.48 and thickness of 0.508 mm.

For comparison, a traditional unit cell having the same dimensions as the proposed slot unit cell but without subsidiary slots is also presented, as shown in Fig. 1(b). The dispersion relations of the fundamental mode for different cases are displayed in Fig. 2(a) where k denotes propagation constant in the x axis. The dispersion curves of the proposed slot unit cell and the traditional slot unit cell significantly both deviate from the light line, indicating that the slot grating structures in Figs. 1(a) and (b) is capable of confining EM waves on the surface, while this deviation is more apparent when the proposed fish-bone topology is employed. The dispersion curves show that the proposed structure obtains lower cutoff frequency implying stronger confinement of surface wave.

The dispersion properties of the proposed SSPPs can be controlled by tailoring the geometrical parameters of the designed grooves. Figures 2(b)-(d) are the dispersion relations of fundamental modes for the proposed slot structure with variance of physical dimensions. For all cases in Figs. 2(b)-(d), when any one parameter (i.e., L_1, D, W_4) is changed, the other parameters of the proposed slot unit cell are kept constant and the same as in Fig. 2(a). As can be seen in Figs. 2(b) and (c), when the subsidiary grooves depth L_1 or period D increases, the dispersion bands are both lowered, indicating stronger confinement ability for SSPPs, while the change of dispersion curve with variance of L_1 is much greater. Additionally, the dependence of the dispersion relation on the pitch between the subsidiary slots W_4 is also studied. As depicted in Fig. 2(d), the dispersion band can be slightly lowered as W_4 decreases. We also analyze the dependence of the dispersion relation on the width of the subsidiary slots W_3 and find its dependence is even weaker than that of W_4.

III. DESIGN OF THE PROPOSED SSPPS-BASED BPF

Based on the dispersion feature analyzed above, by embedding periodic arrangement of the proposed SSPPs unit cells into a waveguide, a corresponding high-frequency stopband is generated. Then a low frequency stopband staring from DC can be evoked by the microstrip-to-slotline transition, where no direct physical connection between microstrip and slotline exists and thus the DC and low frequency signal will be blocked. Finally, an ultra-wideband BPF based on SSPPs using fish-bone slot structure is proposed.

Figure 3(a) is the schematic view of the proposed ultra-wideband BPF consisting of the microstrip-to-slotline transitions and the fish-bone slot unit cells array with the period N of 5. The microstrip line is printed on the top layer of the substrate and used to excite the SSPPs propagating along the fish-bone slot surface which is etched on the bottom layer of the substrate. The material type of metal is selected as copper. The microstrip-to-slotline transition is designed by the microstrip line with a circular pad and the slotline with a circular slot, where two additional fish-bone slot unit

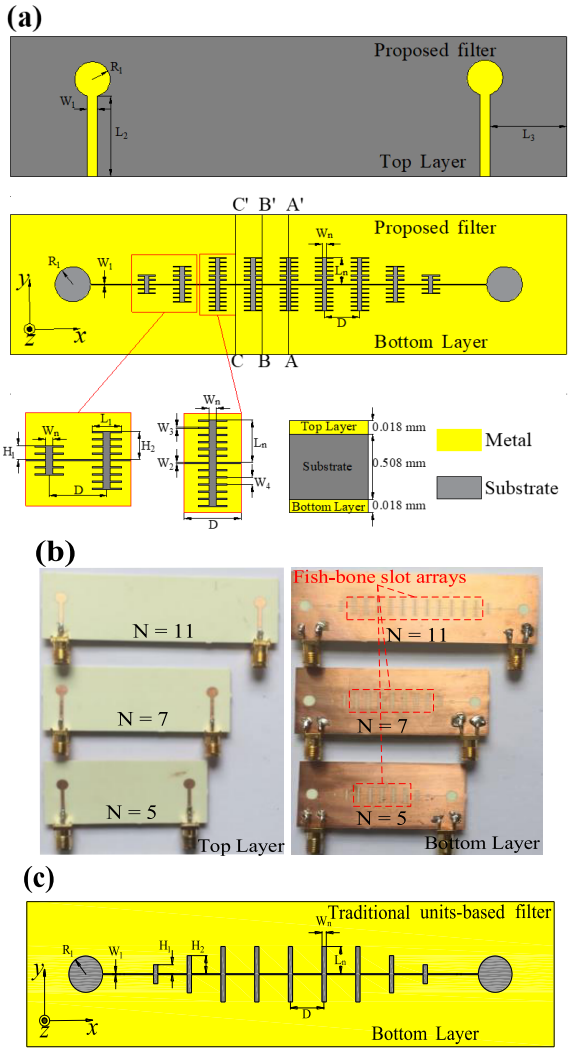

FIGURE 3. (a) Schematic view of the proposed ultra-wideband BPF where $N = 5$. (b) Photographs of the fabricated filters ($N = 5, 7, 11$). (c) Bottom layer of the traditional slot unit cells-based filter, in which the top layer design is the same as that of Fig. 3(a).

cells with different groove depths (i.e., H_1, H_2) are properly designed to improve the impedance matching performance. The length of the microstrip line is L_2, the nearest distance between the microstrip line and the edge of the substrate is L_3, and the radius of the circular pad is equal to that of the circular slot (i.e., R_1). To construct the SSPPs waveguide, N fish-bone slot unit cells are arranged periodically along the x direction to support surface plasmonic wave propagation. In this paper, three cases with different periods (i.e., $N = 5, 7, 11$) are designed, fabricated, as displayed in Fig. 3(b). The fish-bone slot unit cell dimensions are chosen as the same as in Fig. 1(a) where the cutoff frequency is determined to be about 6.8 GHz, while the other parameters R_1, L_2, L_3, H_1, H_2 and W_1 are set as 2 mm, 9.2 mm, 8.6 mm, 1 mm, 2 mm, and 1.1 mm, respectively. For comparison, the traditional slot unit cells-based filter, whose bottom schematic is depicted in Fig. 3(c), is also designed with the same physical parameters as the Fig. 3(a).

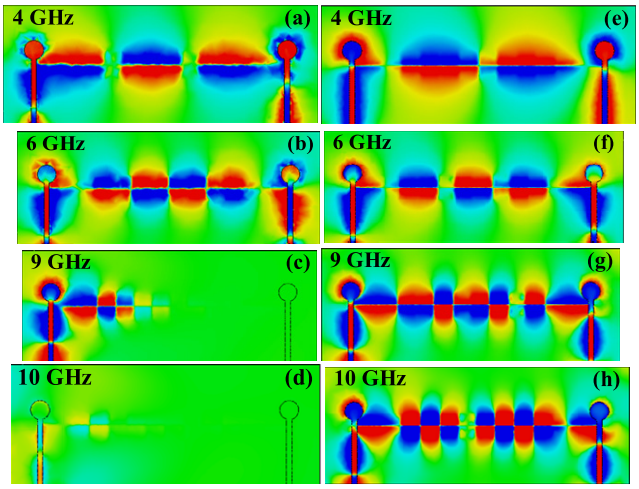

FIGURE 4. 2-D distributions of the z-component E-fields on the observation xy-plane which is 1.5 mm above the top surface of the circuits where $N = 5$. (a)-(d) Proposed filter, and (e)-(h) the traditional structure-based filter at 4 GHz, 6 GHz, 9 GHz, 10 GHz, respectively. Note that all cases are with the same dimensions and color bar in dB scaling.

Figure 4 shows the simulated 2-D distributions of the z-component E-fields. As seen in Figs. 4(a)-(d) corresponding to the proposed ultra-wideband BPF, the observed frequencies are at 4, 6, 9 and 10 GHz, where 4 and 6 GHz are located in the passband, 9 and 10 GHz lie in the stopband. We clearly observe that SSPPs fields can be effectively supported by the proposed slot grating structure when $f = 4$ and 6 GHz, while vanish rapidly along the x direction in the observed plane when $f = 9$ and 10 GHz, proving again that SSPPs modes cannot be supported beyond the cutoff frequency of the proposed fish-bone slot structure. For comparison, the frequencies and positions observed in the traditional unit cell-based filter are completely coincident with those in proposed filter, as exhibited in Figs. 4(e)–(h), which further demonstrate that the proposed fish-bone slot unit cells can support lower cutoff frequency implying higher confinement for SSPPs fields. Moreover, the propagating wavelength on the proposed filter is smaller than that on the traditional structure-based filter, which means the surface wave propagation on the proposed structure is slower and SSPPs-wave confinement ability in the x direction is improved. In other words, to confine surface waves with the constant wavelength, fewer SSPPs unit cells are required with the proposed design compared with that of the traditional one, which is beneficial to the size miniaturization.

To quantitatively describe the confinement phenomena of the proposed and traditional designs, the distributions of electric field amplitudes ($|\mathbf{E}| = [|E_x|^2 + |E_y|^2 + |E_z|^2]^{1/2}$) in the cross-section A-A' along the y-axis direction are calculated as shown in Fig. 5(a). All fields decay exponentially along the y-axis direction, showing the confinement features of SPP modes. As seen in Fig. 5(a), when the groove depth L_n of the proposed/traditional design increases, the confinement will be tightened and thus the field

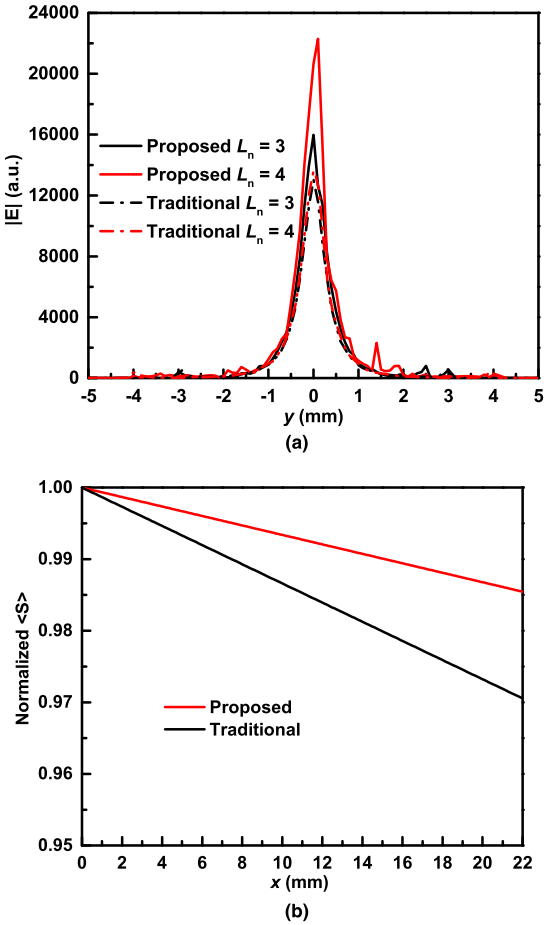

FIGURE 5. (a) Electric field distributions in the cross-section A-A′ and (b) normalized time-averaged power density <S> along the propagation direction of the proposed and traditional designs.

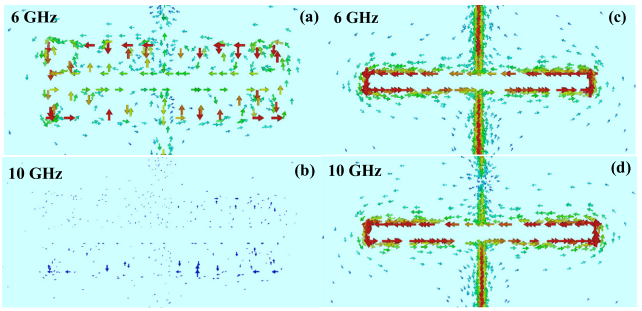

FIGURE 6. Current flow distributions on the bottom surface of the grating structure (i.e., periodic unit cell). (a)-(b) fish-bone slot unit cell, and (c)-(d) the traditional unit cell at 6 GHz and 10 GHz, respectively.

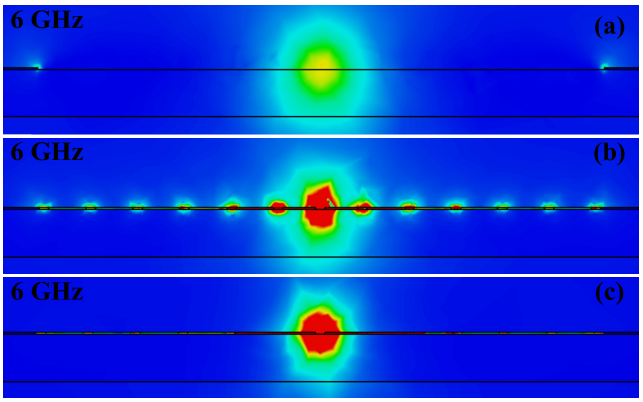

FIGURE 7. Magnitudes of SSPPs energy flows on cross sections of the proposed filter. (a) A-A′, (b) B-B′, and (c) C-C′. All plots have the same color bar in dB scaling. The cross sections of A-A′, B-B′, and C-C′ are indicated in Fig. 3(a).

enhancement increases. On the other hand, when the groove depth L_n keeps constant (i.e., $L_n = 3$ or 4 mm), the proposed design achieves stronger confinement with enhanced fields compared with that of the traditional one. Fig. 5(b) illustrates the normalized time-averaged power density along the propagation direction (i.e., x-axis direction) that lies 0.1 mm above the slot of the traditional and proposed structures. It can be observed that the propagation loss of the proposed design is lower than that of the traditional counterpart.

To further obtain a physical insight into the EM fields confinement of the proposed filter and the traditional structure-based filter, the current flow distributions on the bottom surface of the grating structures for both cases at 4 GHz and 10 GHz are computed, as illustrated in Fig. 6. Compared Fig. 6(a) with Fig. 6(b), the current around the grating structure at 10 GHz is obviously weaker than that at 6 GHz, not mention to some completely vanishing regions, manifesting again the cutoff frequency properties of the proposed slot unit cell. But for the traditional structure-based cases in Figs. 6(c) and (d), there are minor changes for the intensity of currents between 6 GHz and 10 GHz, implying again that the dispersion band of the proposed slot unit cell is lower than that of the traditional one. Additionally, the current path for the proposed slot unit cell is longer than that of the traditional unit cell, resulting in smaller propagating wavelength and slow propagation of SSPPs wave.

To obtain direct observation of the SSPPs modal properties on the proposed filter, Fig. 7 demonstrates the SSPPs energy flows on the cross-sectional cuts at three different locations along the proposed filter at 6 GHz when $N = 5$. It is obviously visualized that the EM fields are tightly confined in the deep sub-wavelength scale around the proposed slot grating structure. The case of Fig. 7(c) shows higher energy level than that of Fig. 7(a), while for the case in Fig. 7(b), the EM energy is localized at many dots in the y direction due to the subsidiary slots of the fish-bone structure.

IV. FREQUENCY RESPONSE AND DISCUSSION

Since the high and low frequency stopbands of the proposed filter is created by the SSPPs unit cells and the microstrip-to-slotline transition, respectively, thus, by tuning the physical parameters of these two structures, the frequency response of the proposed filter is shaped. To validate this tuning ability, full-wave simulations are carried out, as seen in Fig. 8, where L_n, R_1 are swept while all other dimensions remain the same as those in Fig. 3(a). The high frequency edge of the passband shifts upward when groove depth L_n decreases,

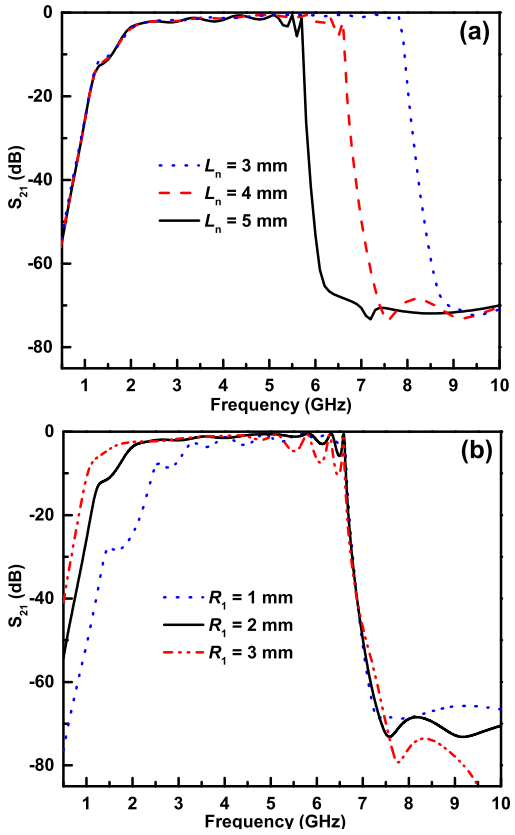

FIGURE 8. S_{21} performance for the proposed BPF with (a) varied groove depth *Ln* and (b) varied radii of the circular pad and slot.

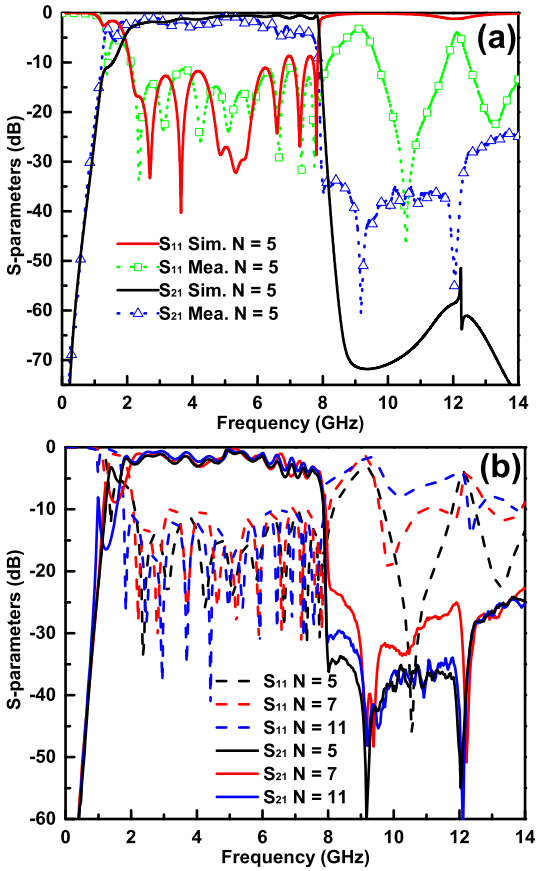

FIGURE 9. Frequency responses of the proposed SSPPs-based BPF. (a) Comparison between the simulated and measured when $N = 5$. (b) Measured S-parameters with the variance of number of fish-bone unit cells *N*.

while the low frequency edge remains constant, which means the geometrical dimensions of the fish-bone slot unit cell is used to determine the cutoff frequency. Besides the groove depth, other parameters of the fish-bone slot unit cell can be also arbitrarily tuned to change the cutoff frequency. Figure 8(b) displays the radius of the circular pad and slot (i.e., R_1) influence on transmission coefficient showing the low frequency edge can be tuned independently by changing R_1. The microstrip-to-slotline transition determines the low frequency edge while having almost no effects on the high frequency edge. The analysis above shows the passband frequency edge of the proposed filter can be controlled separately, which facilitates the design process. Therefore, the center frequency and bandwidth can be both shaped correspondingly.

Figure 9 is the frequency responses of the proposed ultra-wideband BPF, where the measurement was carried out by using Agilent vector network analyzer N5247A. From Fig. 9(a), by passing through two microstrip ends, two transition sections and SSPPs unit cells array, the EM fields still keep high transmissions (S_{21}) and low reflections (S_{11}) within the passband, except some drops with ripples from 4.9 to 7.6 GHz. These ripples may be attributed to the impedance mismatching of transition sections and signal input/output port. The measured results are in agreement with the predicted ones validating the proposed idea. The discrepancy between the simulated and measured *S*-parameters is mainly due to the mutual coupling introduced by the connectors, soldering, and manufacturing tolerance especially in the high frequency. Figure 9(b) is the measured performance comparison between cases with different periods N. These cases have similar S-parameters fluctuation trend in the passband showing that the length of the SSPPs unit cells array is insensitive to the surface wave transmission. In other words, surface wave is capable of propagating on the proposed SSPPs unit cells with low loss, and the insertion loss of the proposed filter mainly results from the other parts rather than the SSPPs unit cells.

V. CONCLUSION

In summary, an SSPPs-based ultra-wideband BPF using fish-bone slot structure is presented and studied. The proposed fish-bone slot unit cell is analyzed by full-wave EM simulation showing lower dispersion band with higher surface wave confinement ability. Based on the proposed slot unit cell and the microstrip-to-slotline transition design, such filter can support low-loss SSPPs transmission with attractive properties such as tight field confinement and tuning ability on bandwidth and center frequency. The proposed SSPPs-based filter is a good candidate for functional plasmonic circuit applications in microwave and terahertz regimes.

REFERENCES

[1] S. A. Maier, *Plasmonics: Fundamentals and Applications*. New York, NY, USA: Springer, 2007.

[2] L. Yin *et al.*, "Subwavelength focusing and guiding of surface plasmons," *Nano Lett.*, vol. 5, no. 7, pp. 1399–1402, Jun. 2005, doi: 10.1021/nl050723m.

[3] J. A. Schuller, E. S. Barnard, W. Cai, Y. C. Jun, J. S. White, and M. L. Brongersma, "Plasmonics for extreme light concentration and manipulation," *Nature Mater.*, vol. 9, no. 3, pp. 193–204, 2010, doi: 10.1038/nmat2630.

[4] J. N. Anker, W. P. Hall, O. Lyandres, N. C. Shah, J. Zhao, and R. P. Van Duyne, "Biosensing with plasmonic nanosensors," *Nature Mater.*, vol. 7, no. 6, pp. 442–453, Jun. 2008, doi: 10.1038/nmat2162.

[5] J. Pendry, "Playing tricks with light," *Sci.*, vol. 285, no. 5434, pp. 1687–1688, Sep. 1999, doi: 10.1126/science.285.5434.1687.

[6] A. C. Jones, "Mid-IR plasmonics: Near-field imaging of coherent plasmon modes of silver nanowires," *Nano Lett.*, vol. 9, no. 7, pp. 2553–2558, Jun. 2009, doi: 10.1021/nl900638p.

[7] J. Prikulis, P. Hanarp, L. Olofsson, D. Sutherland, and M. Käll, "Optical spectroscopy of nanometric holes in thin gold films," *Nano Lett.*, vol. 4, no. 6, pp. 1003–1007, 2004, doi: 10.1021/nl0497171.

[8] J. B. Pendry, L. Martín-Moreno, and F. J. Garcia-Vidal, "Mimicking surface plasmons with structured surfaces," *Science*, vol. 305, pp. 847–848, Aug. 2004, doi: 10.1126/science.1098999.

[9] J. Y. Yin, H. C. Zhang, Y. Fan, and T. J. Cui, "Direct radiations of surface plasmon polariton waves by gradient groove depth and flaring metal structure," *IEEE Antennas Wireless Propag. Lett.*, vol. 15, pp. 865–868, 2015, doi: 10.1109/LAWP.2015.2477877.

[10] M. J. Lockyear, A. P. Hibbins, and J. R. Sambles, "Microwave surface-plasmon-like modes on thin metamaterials," *Phys. Rev. Lett.*, vol. 102, no. 7, p. 073901, 2009, doi: https://doi.org/10.1103/PhysRevLett.102.073901.

[11] X. Shen, T. J. Cui, D. F. Martin-Cano, and J. Garcia-Vidal, "Conformal surface plasmons propagating on ultrathin and flexible films," *Proc. Nat. Acad. Sci. USA*, vol. 110, no. 1, pp. 40–45, 2013, doi: 10.1073/pnas.1210417110.

[12] X. Gao *et al.*, "Ultrathin dual-band surface plasmonic polariton waveguide and frequency splitter in microwave frequencies," *Appl. Phys. Lett.*, vol. 102, no. 15, p. 151912, 2013, doi: https://doi.org/10.1063/1.4802739.

[13] H. C. Zhang, T. J. Cui, Q. Zhang, Y. Fan, and X. Fu, "Breaking the challenge of signal integrity using time-domain spoof surface plasmon polaritons," *ACS Photon.*, vol. 2, no. 9, pp. 1333–1340, 2015, doi: 10.1021/acsphotonics.5b00316.

[14] Z. Han, Y. Zhang, and S. I. Bozhevolnyi, "Spoof surface plasmon-based stripe antennas with extreme field enhancement in the terahertz regime," *Opt. Lett.*, vol. 40, no. 11, pp. 2533–2536, 2015, doi: 10.1364/OL.40.002533.

[15] Q. Zhang, Q. Zhang, and Y. Chen, "Spoof surface plasmon polariton leaky-wave antennas using periodically loaded patches above PEC and AMC ground planes," *IEEE Antennas Wireless Propag. Lett.*, vol. 16, pp. 3014–3017, 2017, doi: 10.1109/LAWP.2017.2758368.

[16] H. C. Zhang, S. Liu, X. Shen, L. H. Chen, L. Li, and T. J. Cui, "Broadband amplification of spoof surface plasmon polaritons at microwave frequencies," *Laser Photon. Rev.*, vol. 9, no. 1, pp. 83–90, Jan. 2015, doi: 10.1002/lpor.201400131.

[17] H. Yi, S.-W. Qu, and X. Bai, "Antenna array excited by spoof planar plasmonic waveguide," *IEEE Antennas Wireless Propag. Lett.*, vol. 13, pp. 1227–1230, 2014, doi: 10.1109/LAWP.2014.2332257.

[18] Y. J. Zhou and B. J. Yang, "Planar spoof plasmonic ultra-wideband filter based on low-loss and compact terahertz waveguide corrugated with dumbbell grooves," *Appl. Opt.*, vol. 54, no. 14, pp. 4529–4533, 2015, doi: https://doi.org/10.1364/AO.54.004529.

[19] Y. J. Zhou, C. Zhang, L. Yang, and Q. Xiao, "Electronically controllable spoof localized surface plasmons," *J. Phys. D, Appl. Phys.*, vol. 50, no. 42, p. 425102, 2017, doi: 10.1088/1361-6463/aa88fe.

[20] Y. J. Zhou and B. J. Yang, "A 4-way wavelength demultiplexer based on the plasmonic broadband slow wave system," *Opt. Exp.*, vol. 22, no. 18, pp. 21589–21599, 2014, doi: https://doi.org/10.1364/OE.22.021589.

[21] B. J. Yang, Y. J. Zhou, and Q. X. Xiao, "Spoof localized surface plasmons in corrugated ring structures excited by microstrip line," *Opt. Exp.*, vol. 23, no. 16, pp. 21434–21442, 2015, doi: 10.1364/OE.23.021434.

[22] M. Z. Hu *et al.*, "Ultra-wideband filtering of spoof surface plasmon polaritons using deep subwavelength planar structures," *Sci. Rep.*, vol. 6, Nov. 2016, Art. no. 37605, doi: 10.1038/srep37605.

[23] D. Zhang, K. Zhang, Q. Wu, X. Ding, and X. Sha, "High-efficiency surface plasmonic polariton waveguides with enhanced low-frequency performance in microwave frequencies," *Opt. Exp.*, vol. 25, no. 3, pp. 2121–2129, 2017, doi: http://dx.doi.org/10.1364/OE.25.002121.

[24] T. Qiu, J. Wang, Y. Li, J. Wang, and S. Qu, "Broadband circulator based on spoof surface plasmon polaritons," *J. Phys. D, Appl. Phys.*, vol. 49, no. 35, p. 355002, 2016, doi: 10.1088/0022-3727/49/35/355002.

[25] X. Gao, L. Zhou, Z. Liao, H. F. Ma, and T. J. Cui, "An ultra-wideband surface plasmonic filter in microwave frequency," *Appl. Phys. Lett.*, vol. 104, no. 19, p. 191603, 2014, doi: https://doi.org/10.1063/1.4876962.

YING JIANG GUO (S'13) received the B.E. degree in electronic engineering from Sichuan University, Chengdu, China, in 2008, and the M.E. degree in electromagnetic field and microwave technology from the University of Electronic Science and Technology of China, Chengdu, in 2011, where he is currently pursuing the Ph.D. degree in electromagnetic field and microwave technology. From 2011 to 2013, he was with the Chengdu Research Institute of Huawei Technology Ltd., where he was involved in the pre-research of ultra-wideband power amplifier, high frequency clock for AD, and 5G communication prototype design. From 2013 to 2014, he was with Sichuan Normal University, where he was a Lecturer. He has filed/granted a number of Chinese patents in microwave circuit and internet of vehicle. His research interests include RF/microwave/mm-wave circuits design, antennas design, and monolithic-microwave integrated circuit applications.

KAI DA XU (S'13–M'15) received the B.S. and Ph.D. degrees in electromagnetic field and microwave technology from the University of Electronic Science and Technology of China, Chengdu, China, in 2009 and 2015, respectively.

From 2012 to 2014, he was a Visiting Researcher with the Department of Electrical and Computer Engineering, Duke University, Durham, NC, USA, under the financial support from the China Scholarship Council. From 2016 to 2017, he was a Post-Doctoral Fellow with the State Key Laboratory of Millimeter Waves, City University of Hong Kong, Hong Kong. He is currently an Assistant Professor with the Institute of Electromagnetics and Acoustics, and also with the Department of Electronic Science, Xiamen University, Xiamen, China. He has authored and co-authored over 80 papers in peer-reviewed journals and conference proceedings. His current research interests include RF/microwave and mm-wave circuits, antenna arrays, and nanoscale memristors.

Dr. Xu is an Editorial Board Member of the *AEÜ-International Journal of Electronics and Communications*. He received the UESTC Outstanding Graduate Award in 2009 and 2015, respectively. He was a recipient of the National Graduate Student Scholarship from the Ministry of Education, China, in 2012, 2013, and 2014, respectively. He is serving as a Reviewer for several IEEE and IET journals, including the IEEE TRANSACTIONS ON MICROWAVE THEORY AND TECHNIQUES, the IEEE TRANSACTIONS ON ELECTRON DEVICES, the IEEE TRANSACTIONS ON COMPUTER-AIDED DESIGN OF INTEGRATED CIRCUITS AND SYSTEMS, the IEEE ANTENNAS AND WIRELESS PROPAGATION LETTERS, the IEEE MICROWAVE AND WIRELESS COMPONENTS LETTERS, the IEEE ACCESS, *IET Microwaves Antennas & Propagation*, and *Electronics Letters*. Since 2017, he has been serving as an Associate Editor for both of the IEEE ACCESS and *Electronics Letters*.

YANHUI LIU (M'15) received the B.S. and Ph.D. degrees in electrical engineering from the University of Electronic Science and Technology of China (UESTC), Sichuan, China, in 2004 and 2009, respectively.

From 2007 to 2009, he was a Visiting Scholar with the Department of Electrical Engineering, Duke University, Durham, NC, USA. Since 2011, he has been with Xiamen University, China, where he is currently a Full Professor with the Department of Electronic Science. He has authored and co-authored over 90 peer-reviewed journal and conference papers. He holds several granted Chinese patents. His research interests include antenna array design, array signal processing, and microwave imaging methods.

Dr. Liu received the UESTC Outstanding Graduate Award in 2004 and the Excellent Doctoral Dissertation Award of Sichuan Province of China in 2012. He is serving as a Reviewer for several international journals, including the IEEE TRANSACTIONS ON ANTENNAS AND PROPAGATION, the IEEE TRANSACTIONS ON GEOSCIENCES AND REMOTE SENSING, the IEEE ANTENNAS AND WIRELESS PROPAGATION LETTERS, the IEEE MICROWAVE AND WIRELESS COMPONENTS LETTERS, *IET Microwave, Antennas & Propagation*, and *Digital Signal Processing*.

XIAOHONG TANG was born in Chongqing, China, in 1962. He received the M.S. and Ph.D. degrees in electromagnetism and microwave technology from the University of Electronic Science and Technology of China (UESTC), Chengdu, China, in 1983 and 1990, respectively.

In 1990, he joined the School of Electronic Engineering, UESTC, as an Associate Professor, and became a Professor in 1998. He has authored or co-authored over 80 technical papers. His current research interests are microwave and millimeter-wave circuits and systems, microwave integrated circuits, and computational electromagnetism.